Title

High contrast optical imaging methods for image guided laser ablation of dental caries lesions

Authors

Lamantia, Nicole R
Tom, Henry
Chan, Kenneth H
et al.

Publication Date

2014-02-18

DOI

10.1117/12.2045683

Peer reviewed

HHS Public Access

Author manuscript

Proc SPIE Int Soc Opt Eng. Author manuscript; available in PMC 2014 April 29.

Published in final edited form as:

Proc SPIE Int Soc Opt Eng. 2014 February 18; 8929: . doi:10.1117/12.2045683.

High contrast optical imaging methods for image guided laser ablation of dental caries lesions

Nicole R. LaMantia, **Henry Tom**, **Kenneth H. Chan**, **Jacob C. Simon**, **Cynthia L. Darling**, and **Daniel Fried**•

University of California, San Francisco, San Francisco, CA 94143-0758

Abstract

Laser based methods are well suited for automation and can be used to selectively remove dental caries to minimize the loss of healthy tissues and render the underlying enamel more resistant to acid dissolution. The purpose of this study was to determine which imaging methods are best suited for image-guided ablation of natural non-cavitated carious lesions on occlusal surfaces. Multiple caries imaging methods were compared including near-IR and visible reflectance and quantitative light fluorescence (QLF). In order for image-guided laser ablation to be feasible, chemical and physical modification of tooth surfaces due to laser irradiation cannot greatly reduce the contrast between sound and demineralized dental hard tissues. Sound and demineralized surfaces of 48 extracted human molar teeth with non-cavitated lesions were examined. Images were acquired before and after laser irradiation using visible and near-IR reflectance and QLF at several wavelengths. Polarization sensitive-optical coherence tomography was used to confirm that lesions were present. The highest contrast was attained at 1460-nm and 1500–1700-nm, wavelengths coincident with higher water absorption. The reflectance did not decrease significantly after laser irradiation for those wavelengths.

Keywords

light scattering; enamel; near-IR imaging; selective laser ablation

1. INTRODUCTION

In order to implement an image-guided approach for selectively removing caries lesions, images of demineralization on tooth surfaces will need to be acquired and subsequently used to guide a laser to selectively ablate those areas. This approach requires the rapid acquisition of high-contrast images of areas of enamel and dentin demineralization that can be input into the laser-scanning system to selectively remove the decay. Lesion areas can then be identified using image analysis routines. Computer control is now feasible due to the recent advances in compact high-speed laser scanning technology such as MEMS (Micro-Electro-Mechanical Systems) mirrors and miniature galvanometer “galvo” based scanners. One approach is to remove the lesion layer by layer, i.e. image the lesion then scan the laser and

•Contact Author: daniel.fried@ucsf.edu.

remove an outer layer of the lesion, then re-image and scan again repeating that process until the lesion is completely removed. High contrast images can be acquired using the most promising caries imaging systems, namely fluorescence and near-IR imaging and those images will be used to program the laser scanning system to position the laser-beam over the area of the tooth surface to be ablated.

A potential concern, that is fundamental to the success of this approach, is that thermal modification of sound and demineralized tooth surfaces by the laser, may interfere with the ability to acquire useful images of the laser irradiated surfaces. The performance of each of the image modalities is expected to vary due to variations in surface topography, presence of stain, degree of hydration and increased surface scattering caused by roughening of the surface by the laser. Therefore, it is necessary to measure the lesion contrast both before and after laser ablation has been initiated. The purpose of this study was to measure the reduction in contrast between sound and demineralized enamel after surface modification by a carbon dioxide laser for visible and near-IR reflectance and quantitative light fluorescence (QLF). The imaging method that yields the highest pre-and post ablation contrast is most suitable for image-guided ablation of occlusal caries lesions.

Fluorescence has been combined with laser ablation for caries removal. Eberhard et al. [1–3] have combined laser ablation with an Er:YAG laser with red fluorescence (655-nm excitation, 680+ detection) and they claim this combination can be used to selectively remove infected dentin. Lennon and Buchalla et al. [4–6] have developed red fluorescence aided caries excavation (FACE) for use with the conventional handpiece and claim it has superior performance than conventional excavation, caries detector dyes and chemomechanical removal; however they use 370-nm excitation and 530-nm+ detection. Stains will also interfere with fluorescence.

Tao et al. [7] created patterned lesions on blocks of bovine enamel and demonstrated that images of the patterned lesions acquired using near-IR transillumination measurements could be used to guide a 9.3-μm CO_2 laser for highly selective laser ablation.

Recent studies suggest that near-IR reflectance imaging is ideally suited for acquiring high-contrast images for image guided ablation due to the weak light scattering from sound enamel and the lack of interference from stain [8–10]. Stains which greatly interfere with visible reflectance and QLF measurements of lesion contrast, do not interfere at near-IR wavelengths. Stains cause the lesion areas to appear darker, not lighter, in the visible range, and the stained areas do not represent the areas of demineralization. This is why visible reflectance measurements are of limited effectiveness in the occlusal surfaces [11, 12] and are not suitable for guiding laser ablation. In addition, the near-IR has high transmission through zinc selenide optics which is an important advantage when working with CO_2 lasers. A comparison of QLF, near-IR (1310-nm) and visible cross-polarization reflectance imaging for early demineralization, indicated that the highest lesion contrast was for near-IR reflectance [13]. Cross-polarization imaging is useful for removing the strong specular reflection “glare” from sound surfaces during reflected light imaging. More recent reflectance measurements at 1460-nm yielded even higher contrast than other near-IR wavelengths because the peak in water absorption at this wavelength reduces the intensity of

backscattered light from the underlying dentin [14, 15]. Near-IR measurements also manifest a greater range in contrast values with increased severity of demineralization and can better represent variations in the lesion severity [16].

2. MATERIALS AND METHODS

Forty-eight human teeth with non-carious occlusal surfaces were collected (Exempt, IRB not required) and sterilized with gamma radiation. All teeth were mounted in black orthodontic acrylic blocks. Samples were stored in a moist environment of 0.1% thymol to maintain tissue hydration and prevent bacterial growth. Teeth were examined visually and then scored according to the ICDAS classification system. Only teeth with scores of 1 & 2 were used. The CO_2 laser was used to cut three 2 × 2 mm square windows with the lesion in the center box as shown in Fig. 1. The outlines of three windows were cut on the occlusal surface of each tooth using a CO_2 laser. The channels cut by the laser also serve as reference points for serial sectioning and are sufficiently narrow to not interfere with calculations of the image contrast. The lesion contrast was compared for visible reflectance 400–650-nm, near-IR reflectance imaging at 900–1700-nm, 1300, 1460 and 1500–1700 nm and for fluorescence imaging with 405-nm (green-collagen) excitation and for emission at wavelengths greater than 500-nm. The lesion contrast was calculated by measuring the ratio of the intensity of a lesion area vs. sound area (differential radiance) for each of the samples before ablation and after ten ablation scans have been completed. Polarization sensitive optical coherence tomography (PS-OCT) was used to both screen for tooth selection and serve as a surrogate gold standard to identify the areas of demineralization. Samples were air dried for 5 seconds prior to acquiring images. The 48 teeth were separated into two groups. The first group (n=28) was used for comparison of visible reflectance (400–650-nm), near-IR reflectance (900–1700-nm) and fluorescence (QLF). The second group (n=20) was used for comparison of different near-IR reflectance wavelengths 900–1700-nm, 1300, 1460 and 1500–1700 nm.

2.1 Near-IR Cross Polarization Reflectance Images

In order to acquire reflected light images, NIR light was directed towards the occlusal surface through a broadband fused silica beamsplitter (1200–1600-nm) Model BSW12 (Thorlabs, Newton, NJ) and the reflected light from the tooth was transmitted by the beamsplitter to the imaging camera. Crossed polarizers were placed after the light source and before the detector and used to remove specular reflection (glare) that interferes with measurements of the lesion contrast. The near-IR reflectance images were captured using a 320 × 240 element InGaAs area camera SU320-KTSX from Sensors Unlimited (Princeton, NJ) sensitive from 900–1700-nm with a 25-μm pixel pitch. Reflectance measurements were taken for three spectral bands using two bandpass filters and a longpass filter. The band pass filters were BP1300-90 and BP1460-85 from Spectrogon (Parsippany, NJ) and the 1500-nm long-pass filter was the FEL 1500 from Thorlabs (Newton, NJ). The optical layout is shown in Fig. 2.

2.2 QLF (Fluorescence) Measurements

To collect QLF images, a GaN laser diode module “Blu-Ray” (λ=405-nm) operating with 60-mW (Photonic Products, UK) was used as an excitation source. A 500-nm long-pass

filter #C47-616 (Edmund Scientific, Barrington, NJ) and a DFK 31AF03 FireWire camera (resolution 1024 × 768) from the Imaging Source (Charlotte, NC) equipped with an Infinimite lens (Infinity Photooptical, Boulder, CO), were used to image the fluorescence from the surface at wavelengths longer than 500-nm. Imaging was carried out in the dark to avoid the interference of ambient light.

2.3 Visible Cross Polarization Reflectance Images

Visible Reflectance images were acquired using an Ocean Optics fiber-coupled tungsten-halogen lamp (Model HL-2000-FHSA) with a DFK 31AF03 FireWire camera outfitted with a MiniInfinimite lens. The sensor's built in near-IR filter limits the spectral sensitivity to 400 – 650-nm. The light source was equipped with a linear polarizer and the camera was equipped with a second linear polarizer oriented orthogonal relative to the initial polarizer (crossed polarizers) in order to remove specular reflection from the tooth surface.

2.4 Laser Irradiation

Samples were irradiated using an industrial CO_2 marking laser, Impact 2500 from GSI Lumonics (Rugby, United Kingdom) operating at a wavelength of 9.3 μm. The laser was custom modified to produce a Gaussian output beam (single spatial mode) and a pulse duration between 10–15-μs. The laser energy output was monitored using a power meter EPM 1000, Coherent-Molectron (Santa Clara, CA), and the Joulemeter ED-200 from Gentec (Quebec, Canada). A sound and lesion box on each tooth was irradiated by the laser. Computer-controlled XY galvanometers 6200HM series with MicroMax Series 671 from Cambridge Technology, Inc. (Cambridge) were used to scan the laser beam over the sample surfaces. A repetition rate of 100-Hz was used with point to point scanning with an overlap of 50-μm focused to a spot size of ~350-μm using a ZnSe scanning lens of 90-mm focal length for an incident fluence of 20 J/cm^2 (19 mJ per pulse). Surfaces were scanned twice by the laser to remove approximately 100–150-μm of sound and demineralized enamel. A pressure air- actuated fluid spray delivery system consisting of a 780S spray valve, a Valvemate 7040 controller, and a fluid reservoir from EFD, Inc. (East Providence, RI) was used to provide a uniform spray of fine water mist onto the tooth surfaces at 2 mL/min.

The reference boxes were cut into the samples using a spot size of 200-μm, an overap of 50-μm and a pulse repetition rate of 50-Hz with 30-mJ per pulse.

2.5 PS-OCT System

An all-fiber-based optical coherence domain reflectometry (OCDR) system with polarization maintaining (PM) optical fiber, high-speed piezoelectric fiber-stretchers and two balanced InGaAs receivers that was designed and fabricated by Optiphase, Inc., Van Nuys, CA. This two-channel system was integrated with a broadband superluminescent diode (SLD) Denselight (Jessup, MD) and a high-speed XY-scanning system (ESP 300 controller and 850G-HS stages, National Instruments, Austin, TX) for *in vitro* optical tomography. The spectral output of the 15-mW SLD was centered at 1317 nm with a spectral bandwidth full-width at half-maximum (FWHM) of 84 nm. This configuration provided a lateral resolution of approximately 20 μm and an axial resolution of 9 μm in air.

The system is described in greater detail in reference [17]. The PS-OCT scans were used to confirm the presence of the occlusal lesions.

2.6 Image Analysis and Statistics

Three boxes (2×2 mm) were cut in the occlusal surface (Fig. 1). The left box contained sound enamel, the pit or groove containing the demineralization was contained within the middle box, and the right box contained sound enamel that was ablated by the laser. Contrast values were calculated for each specific region of interest (ROI). Images were analyzed using the image analysis package, IgorPro (Wavemetrics, Lake Oswego, OR). The free form polygon tool in Igor Pro was used to measure intensities encompassing only the lesion (or only the sound, or only ablated) of perceived demineralization by the imaging system using a similar approach to our prior study [16]. Near-IR and visible-light reflectance contrast ratios were produced using the equation $(I_L - I_S)/I_L$, because the increased scattering from demineralized tissue increases the reflectivity. QLF reflectance contrast measurements have the opposite contrast and were calculated using the equation $(I_S - I_L)/I_S$, because decreased fluorescence emission from demineralized tissue reduces the intensity from those areas. The left (sound) box and the central (lesion) box were used for both the preand post contrast calculations. Both the left (sound) box and the central (lesion) box were irradiated by the laser (post contrast) The QLF measurements have the reverse contrast, i.e., the intensity in sound areas is higher than for the lesion areas.

A repeated measures one-way analysis of variance (ANOVA) followed by the Tukey-Kramer post-hoc multiple comparison test was used to compare groups employing Prism software (GraphPad, San Diego, CA).

3. RESULTS AND DISCUSSION

Images of a tooth from the first sample group before and after laser irradiation are shown in Fig. 3. After laser modification of the enamel surface the mean contrast values were reduced by 67% for fluorescence, 28% for visible reflectance and the contrast values increased by 1% for near-IR. The reduction in the contrast for QLF was statistically significant ($P < 0.05$). Images of the window areas are shown for the second group (near-IR wavelengths) before and after laser irradiation in Figure 4. Table I lists the contrast values for both sample groups. The mean contrast values for the near-IR groups are also plotted in Fig. 5.

The contrast before and after laser irradiation was also measured for samples with a wet surface. Surface water has a profound effect on the lesion contrast. Near-IR wavelengths coincident with higher water absorption such as 1460-nm and 1500–1700-nm are particularly sensitive to surface water and the contrast became inverted from high positive values for dry surfaces to negative values for wet surfaces.

Lesion contrast was significantly higher ($p<0.05$) for near-IR reflectance versus visible reflectance and fluorescence both before and after laser irradiation. The highest contrast was attained at 1460-nm and 1500–1700-nm, wavelengths coincident with higher water absorption. The reflectance did not decrease significantly after laser irradiation for those wavelengths. Near-IR wavelengths are also insensitive to stains on tooth surfaces which is a

major advantage over visible reflectance and florescence. Water is a concern and images will have to be acquired of dry surfaces. This can be easily accomplished with a pulsed air/water cooling system that is already used for hard tissue laser ablation systems.

In conclusion, near-IR reflectance at wavelengths coincident with higher water absorption appear best suited for image guided ablation of dental caries lesions.

ACKNOWLEDGMENTS

This work was supported By NIH/NIDCR Grants R01-DE14698 and R01-DE17869. The authors would like to thank Michal Staninec and Robert Lee for their help with this study.

REFERENCES

1. Eberhard J, Bode K, Hedderich J, Jepsen S. Cavity size difference after caries removal by a fluorescence-controlled Er:YAG laser and by conventional bur treatment. Clinical Oral Investigations. 2008; 12(4):311–318. [PubMed: 18500542]
2. Eberhard J, Eisenbeiss AK, Braun A, Hedderich J, Jepsen S. Evaluation of selective caries removal by a fluorescence feedback-controlled Er:YAG laser in vitro. Caries Res. 2005; 39(6):496–504. [PubMed: 16251795]
3. Jepsen S, Acil Y, Peschel T, Kargas K, Eberhard J. Biochemical and morphological analysis of dentin following selective caries removal with a fluorescence-controlled Er:YAG laser. Lasers Surg. Med. 2008; 40(5):350–357. [PubMed: 18563782]
4. Lennon AM. Fluorescence-aided caries excavation (FACE) compared to conventional method. Operative dentistry. 2003; 28(4):341–345. [PubMed: 12877417]
5. Lennon AM, Attin T, Buchalla W. Quantity of remaining bacteria and cavity size after excavation with FACE, caries detector dye and conventional excavation in vitro. Operative dentistry. 2007; 32(3):236–241. [PubMed: 17555174]
6. Lennon AM, Attin T, Martens S, Buchalla W. Fluorescence-aided caries excavation (FACE), caries detector, and conventional caries excavation in primary teeth. Pediatr Dent. 2009; 31(4):316–319. [PubMed: 19722440]
7. Tao YC, Fried D. Near-infrared image-guided laser ablation of dental decay. Journal of Biomedical Optics. 2009; 14(5):054045. [PubMed: 19895146]
8. Bühler CM, Ngaotheppitak P, Fried D. Imaging of occlusal dental caries (decay) with near-IR light at 1310-nm. Optics Express. 2005; 13(2):573–582. [PubMed: 19488387]
9. Jones G, Jones RS, Fried D. Transillumination of interproximal caries lesions with 830-nm light. SPIE Proceeding. 2004; Vol. 5313:17–22.
10. Jones RS, Huynh GD, Jones GC, Fried D. Near-IR Transillumination at 1310-nm for the Imaging of Early Dental Caries. Optics Express. 2003; 11(18):2259–2265. [PubMed: 19466117]
11. Borsboom PCF, ten Bosch JJ. Fiber-optic scattering monitor for use with bulk opaque material. Appl. Optics. 1982; 21(19):3531–3535.
12. ten Bosch JJ, van der Mei HC, Borsboom PCF. Optical monitor of in vitro caries. Caries Res. 1984; 18:540–547. [PubMed: 6593126]
13. Wu J, Fried D. High contrast near-infrared polarized reflectance images of demineralization on tooth buccal and occlusal surfaces at λ = 1310-nm. Lasers Surg. Med. 2009; 41(3):208–213. [PubMed: 19291753]
14. Chung S, Fried D, Staninec M, Darling CL. Multispectral near-IR reflectance and transillumination imaging of teeth. Biomed. Opt. Express. 2011; 2(10):2804–2814. [PubMed: 22025986]
15. Fried WA, Darling CL, Chan K, Fried D. High Contrast Reflectance Imaging of Simulated Lesions on Tooth Occlusal Surfaces at Near-IR Wavelengths. Lasers Surg. Med. 2013; 45:533–541. [PubMed: 23857066]

16. Simon JC, Chan KH, Darling CL, Fried D. Multispectral near-IR reflectance imaging of simulated early occlusal lesions: Variation of lesion contrast with lesion depth and severity. Lasers in Surg. Med. 2014 in press (early view).

17. Fried D, Xie J, Shafi S, Featherstone JDB, Breunig T, Lee CQ. Early detection of dental caries and lesion progression with polarization sensitive optical coherence tomography. J. Biomed. Optics. 2002; 7(4):618–627.

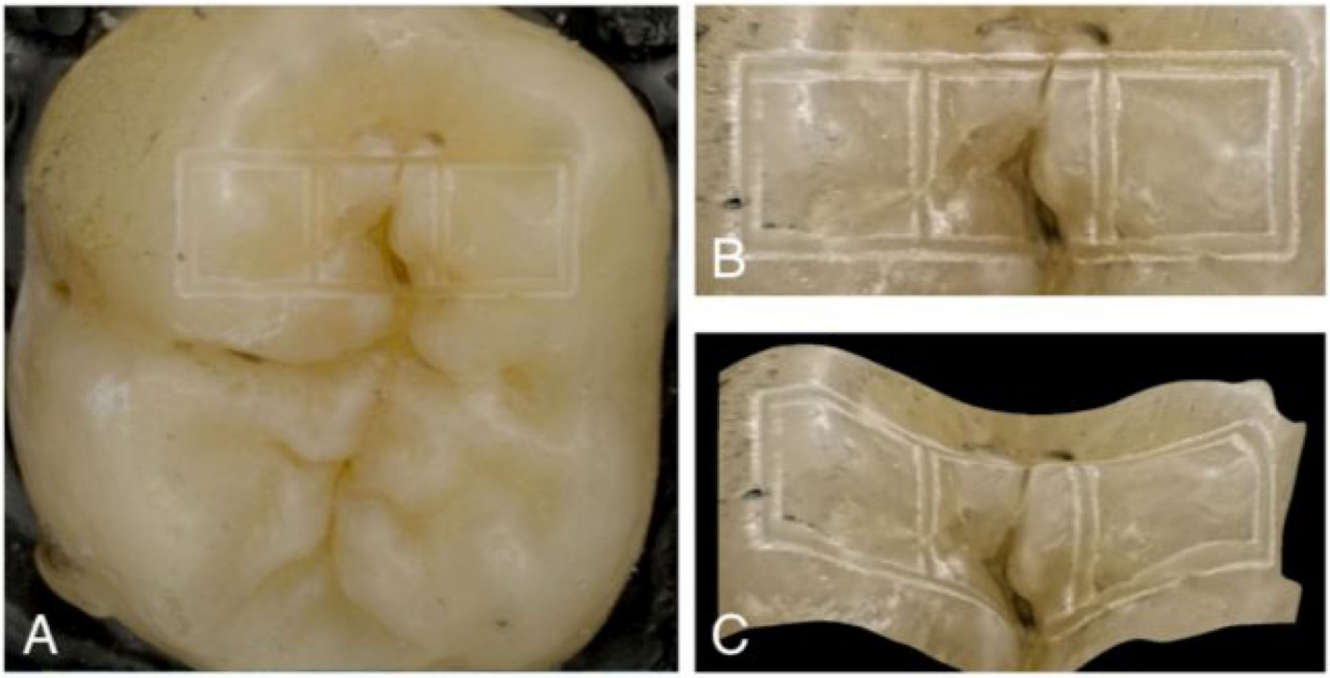

Fig. 1.

Whole tooth (A) showing three windows. Depth composition (B) and 3D (C) images of the windows were taken with a digital microscope. The left box is a sound area which was ablated by the laser. The central box contains a lesion and it was also ablated. The right box contains a 2nd sound area that was not ablated by the laser.

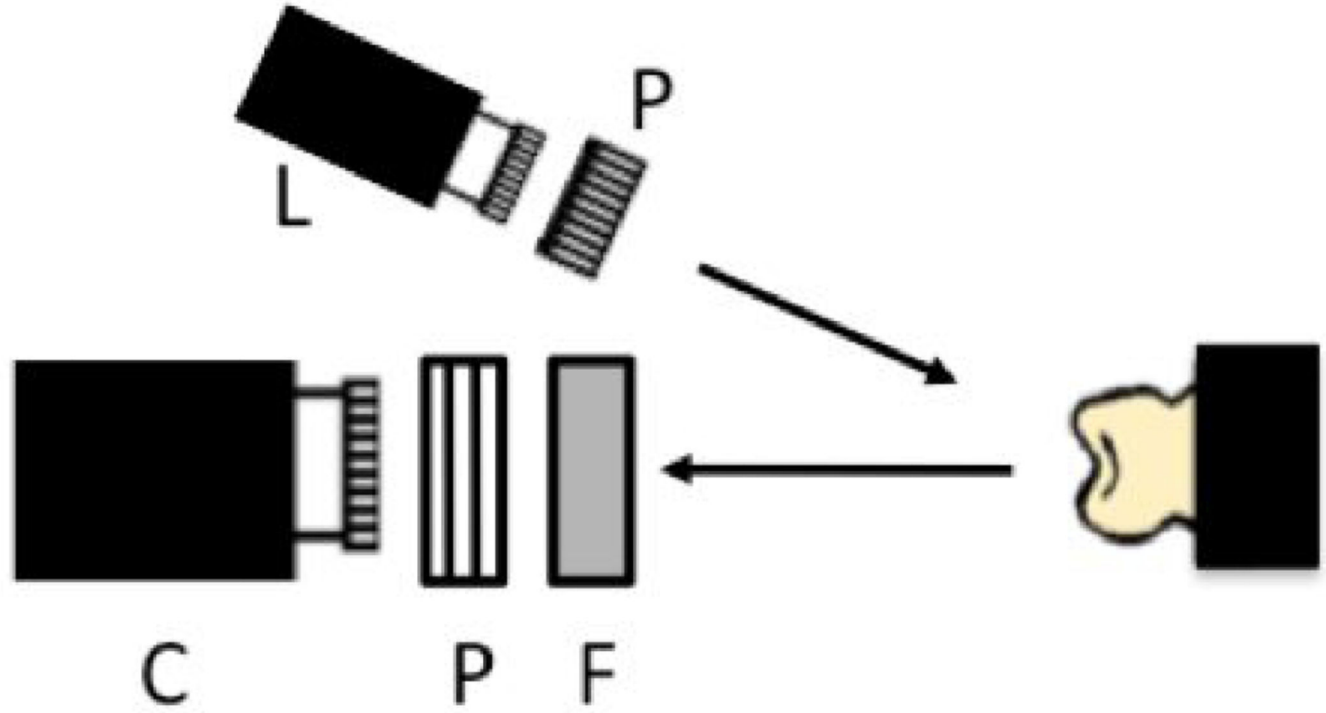

Fig. 2.
Optical layout showing the camera (C), light source (L), polarizers (P) and filter (F) and the position of the tooth.

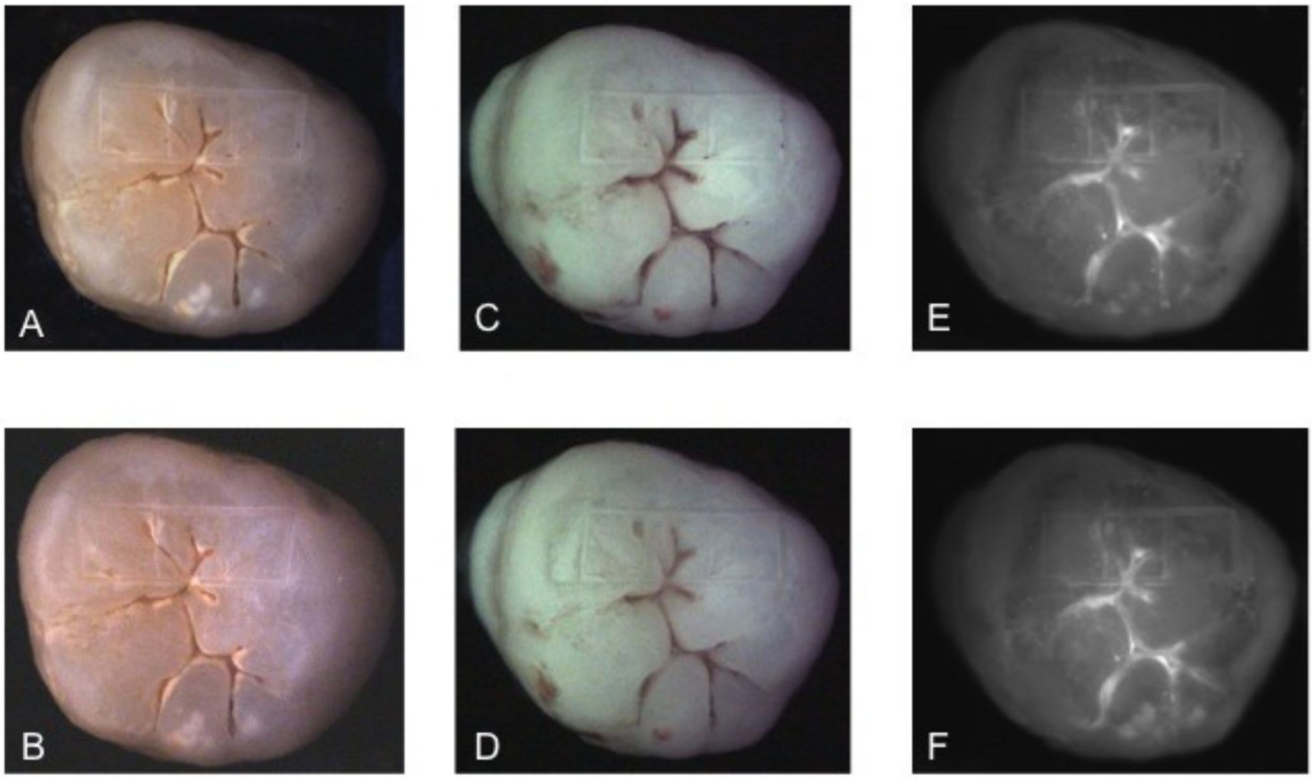

Fig. 3.

Visible reflectance images before (A) and after (B) laser ablation, QLF images before (C) and after (D) ablation and near-IR reflectance (900–1700-nm) before (E) and after (F) ablation are shown.

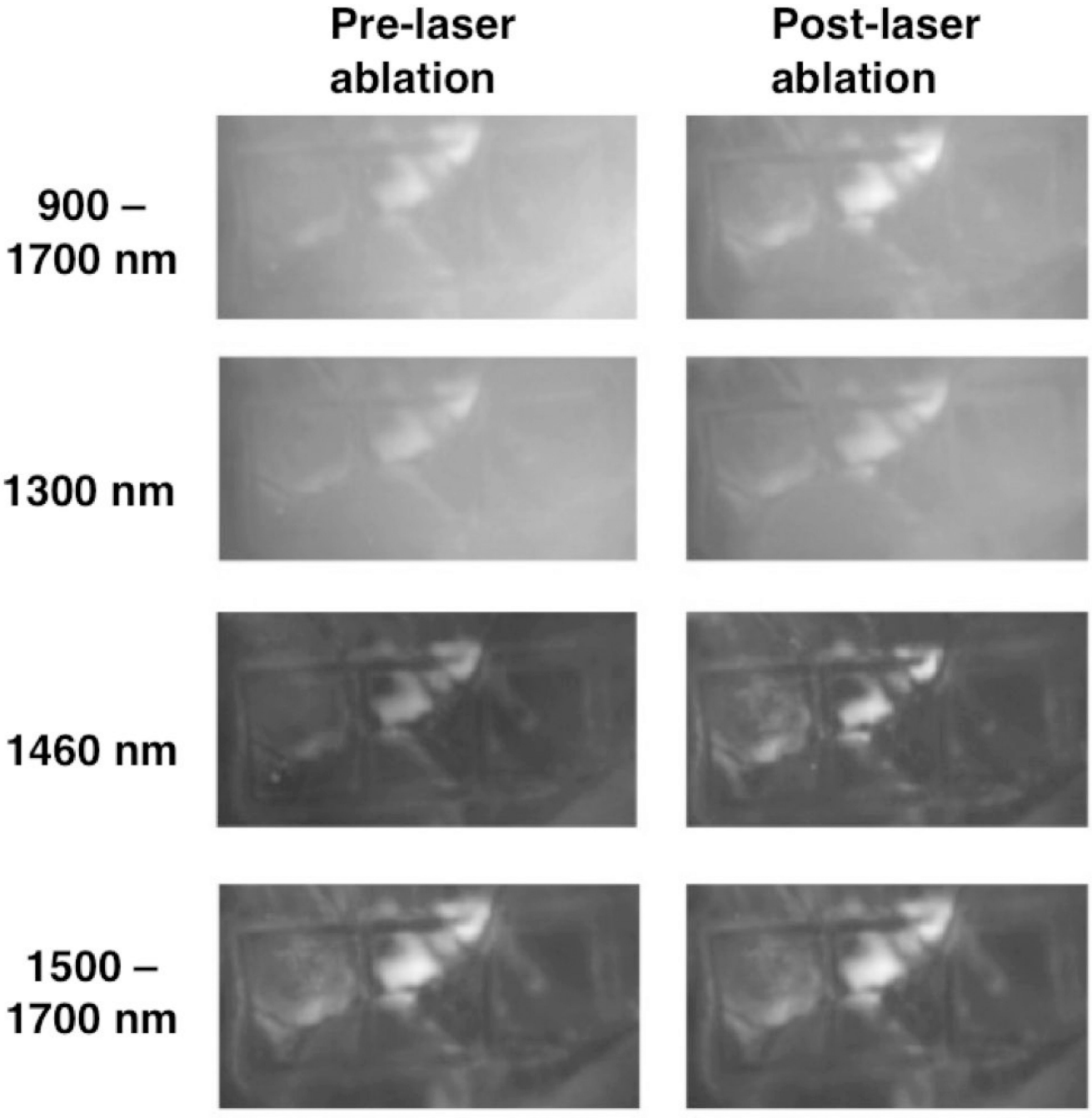

Fig. 4.
Near-IR reflectance images taken of the windows before and after laser ablation using different near-IR spectral bands.

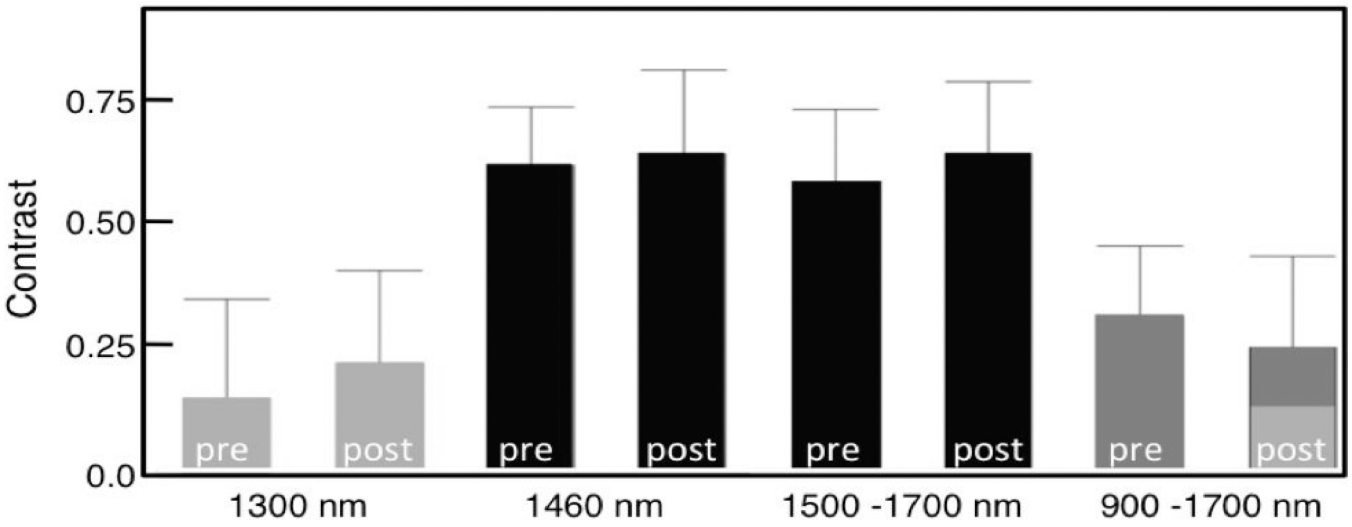

Fig. 5.

The mean lesion contrast values for the near-IR group (n=28) before (pre) and after ablation (post). Columns with the same color are statistically similar (P>0.05).

Table I

The mean lesion contrast values for the two groups of samples, the near-IR reflectance group (n=28) and the fluorescence and visible and near-IR reflectance group (n=20). Near-IR is from 900–1700-nm, 1500 is from 1500–1700 nm and (+) is before laser irradiation and (−) is after laser irradiation. Columns with the same letter within each of the two groups are statistically similar (P>0.05).

Wavelength	**+1300**	**−1300**	**+1460**	**−1460**	**+1500**	**−1500**	**+near-IR**	**−near-IR**
Mean (sd)	0.15(0.22)	0.23(0.21)	0.67(0.13)	0.70(19)	0.63(0.16)	0.69(0.16)	0.33(0.16)	0.27(0.20)
Significance	a	a,c	b	b	b	b	c	a,c
Wavelength	**+ vis**	**−vis**		**+QLF**	**−QLF**		**+near-IR**	**−near-IR**
Mean (sd)	0.15(0.31)	0.11(0.24)		−0.32(0.20)	−0.12(0.21)		0.52(37)	0.53(0.40)
Significance	a	a					b	b